Temporary stratification promotes large greenhouse gas emissions in a shallow eutrophic lake

Thomas A Davidson[1, 2], Martin Søndergaard[1, 2, 3], Joachim Audet[1, 2], Eti Levi[1], Chiara Esposito[1, 2], Tuba Bucak Onay[1], Anders Nielsen[1,4].

[1] Lake Ecology, Department of Ecoscience, Aarhus University, Denmark

[2] WATEC Aarhus University Centre for Water Technology, Aarhus University, Denmark

[3.] Sino-Danish Centre for Education and Research (SDC), Beijing, China

[4.] WaterITech Aps, Døjsøvej 1, 8660 Skanderborg, Denmark

Corresponding author: Thomas A Davidson, Department of Ecoscience, Aarhus University, C. F. Møllers Alle 4-6, DK-8000 Aarhus C, Denmark, e-mail: thd@ecos.au.dk

Abstract

Shallow lakes and ponds undergo frequent temporary thermal stratification. How this affects greenhouse gas (GHG) emissions is moot, with both increased and reduced GHG emissions hypothesised. Here, weekly estimation of GHG emissions, over growing season from May to September, were combined with temperature and oxygen profiles of an 11 hectare temperate shallow lake to investigate how thermal stratification shapes GHG emissions. There were three main stratification periods with profound anoxia occurring in the bottom waters upon isolation from the atmosphere. Average diffusive emissions of methane (CH_4) and nitrous oxide (N_2O) were larger and more variable in the stratified phase, whereas carbon dioxide (CO_2) was on average lower, though these differences were not statistically significant. In contrast, there was a significant, order of magnitude, increase in CH_4 ebullition in the stratified phase. Furthermore, at the end of the period of stratification, there was a large efflux of CH_4 and CO_2 as the lake mixed. Two relatively isolated turnover events were estimated to have released the majority of the CH_4 emitted between May and September. These results demonstrate how stratification patterns can shape GHG emissions and highlight the role of turnover emissions and the need for high frequency measurements of GHG emission which are required to accurately characterise emissions, particularly from temporarily stratifying lakes.

Keywords: Climate change; lake stratification; methane; carbon dioxide; nitrous oxide; climate feedbacks

1. Introduction

Fresh waters are key sites for the processing of greenhouse gases (GHG), methane (CH_4), carbon dioxide (CO_2) and nitrous oxide (N_2O). Shallow lakes, in particular, have been identified as hot spots of CH_4 release, particularly when ebullition is taken into account (Davidson et al., 2018; Aben et al., 2017). The certainty that fresh waters are large emitters of GHGs contrasts with the uncertainties associated with the quantities emitted and this is in large part due to historical paucity of measurements (Cole, 2013). A recent study identified the highly variable emissions from lakes and ponds (Rosentreter et al., 2021). Whilst different morphometric features and chlorophyll-a explained some of the emission patterns (Deemer and Holgerson, 2021), it is also clear that a dearth of measurement combined with these highly variable emissions makes determining the drivers and controls of those emissions a challenge, which in turn makes predicting future emissions difficult.

The current and future effects of climate change on lakes in general and on their GHG emissions are relevant questions as there is potential for positive feedbacks and synergies with other human impacts such as eutrophication (Davidson et al., 2018; Beaulieu et al., 2019; Delsontro et al., 2016; Meerhoff et al., 2022). Taking a broad metabolic theory of ecology approach, temperature increases should promote methanogenesis and shift the balance from primary production to respiration increasing CO_2 emission at cellular and ecosystem scale (Yvon-Durocher et al., 2010). However, empirical and experimental data indicate that temperature is not the sole control of primary production and methanogenesis. In particular, eutrophication, and the promotion of large algal crop, has been associated with increased emissions of CH_4 and N_2O (Delsontro et al., 2016) both by diffusion and ebullition (Zhou et al., 2019). Furthermore, in what is globally the most abundant lake type, small shallow lakes, where macrophytes can colonise large areas of the lake bed, trophic state and the dominance of submerged plants or algae may be more important than temperature in shaping GHG dynamics (Davidson et al., 2015; Davidson et al., 2018; Bastviken et al., 2023).

Climate change effects on lakes are not limited to increases in average temperatures and lengthening of the growing season. Increases in both the frequency and intensity of heat waves are predicted, which will promote the warming of surface waters and in turn make permanent and temporary thermal stratification of lakes more likely (Woolway and Merchant, 2019), even in lakes typically classified as non-stratifying (Kirillin and Shatwell, 2016). A recent study Holgerson et al. (2022) identified stratification and mixing patterns in small water bodies, with permanent summer stratification common and frequent mixing occurring in larger standing waters (>4 ha) lakes. Such periods of stratification and mixing events are likely to have profound effects on GHG dynamics. Emissions of gases, in particular CH_4, that accumulate in the isolated bottom waters of a stratified lake, occurs upon mixing and can make very significant contributions to cumulative emissions (Schubert et al., 2012). High-resolution studies of sites that undergo temporary stratification are rare. Though Søndergaard et al. (2023b), recently showed how stratification shapes patterns and processes across the entire ecosystem, including short term effects on dissolved GHG concentration in bottom and surface waters. In terms of its effects on GHG dynamics, there are potentially antagonistic processes at work in a stratified lake. On the one hand the 'shield effect' results in lower temperatures at the sediment surface slowing down metabolic processes that scale with temperature, i.e. methanogenesis and mineralization of organic carbon (C), reducing emission and promoting C burial. On the other hand, anoxia at the sediment surface may shift processes towards fermentation, increasing the proportion and total amount of CH_4 produced and perhaps reducing C burial (Bartosiewicz et al., 2019). Recent work combining empirical observations and models has suggested that shielding effects are larger than the anoxia effects and that stratification, in general, increases C burial and reduces GHG emissions (Bartosiewicz et al., 2015). The stratification induced isolation of bottom waters was reported to lead to reduced ebullition of CH_4 and a shift to diffusive pathways (Bartosiewicz et al., 2015. It might, however, be predicted that in shallow lakes stratification would lead to much larger CH_4 release as anoxic conditions would limit CH_4 oxidation by CH_4 oxidizing bacteria (MOBs) (Bastviken et al., 2008). There may also be other factors with the potential to increase GHG emission, such as sediment

88 organic content and lake trophic status (Delsontro et al., 2016), which may interact with stratification
89 patterns in shaping GHG emissions.
90
91 In this study, we used data from a shallow lake with high frequency measurements of temperature profiles
92 combined with weekly measurements of dissolved gas concentrations in the surface and bottom waters
93 and continuous measurement of ebullitive emissions of CH_4 to track the effects of lake stratification on
94 GHG emissions. The key question was how ebullitive and diffusive fluxes of the key GHGs: CH_4, CO_2
95 and N_2O respond to temporary thermal stratification.
96

97 # 2. Materials and methods.

98 ## 2.1 Study site

99 Ormstrup lake, located in Denmark (lat 56.326°, lon 9.639°) (Fig.1) (depth map with GHG sampling
100 locations), is an 11 ha, shallow lake (average depth 3.4 m), with a maximum depth of 5.5 m, and with a
101 relatively long hydraulic retention time (> 1 year). The lake is eutrophic with high TP and chlorophyll-a
102 (Table 1; Søndergaard et al., 2022) with very sparse occurrence of submerged plants.
103

104 ## 2.2 Depth profiling and high frequency measurements

105 In June 2020, a Nexsens (NexSens Technology, Fairborn, OH, USA) CB-450 data buoy system
106 (https://www.nexsens.com/pdf/CB450_datasheet.pdf) was deployed at the deepest point of the lake
107 equipped with a Nexsens TS210 thermistor string https://www.nexsens.com/pdf/TS210_datasheet.pdf)
108 with temperature nodes measuring at 4 levels; one sensor “in air”, ca. 5 cm above the water surface, (but
109 shielded from direct light), and three sensors at -1, -2, -3 meters, respectively relative to the water surface.
110 In addition two Aqua TROLL 500 (In-Situ, Fort Collins, CO, USA) multi-sondes were mounted near the
111 surface (-1.0 meters) and at deeper water depth (-3.8 meters). The near surface and deeper water sonde

were configured with sensors to measure dissolved oxygen (DO) and water temperature (Tw). The optical sensors were calibrated according to manufacture guidelines and checked on a weekly basis.

The optical sensors of the Aqua TROLL 500 have a built-in wiper mechanism to clean sensor heads to hamper bio-fouling. The wiper function was enabled to perform cleaning in sync with sensor measurements, hence every 15 minutes. In addition, manual cleaning of sensor heads was done every week, while routine manual field monitoring was carried out at the lake. Prior to the deployment of the buoy, and as a validation exercise for the buoy data, weekly manual profiles of DO and Tw were collected at the deepest point.

Periods of stratification and depth of the thermocline were defined using the r package rlakeanalyzer (Winslow et al., 2019) based on the density gradient of the water column from the weekly manual profiling of the system. During periods of defined as stratified, there were partial mixing events where the depth of the thermocline changed and there was some mixing of the sub epilimnetic water and the surface waters, whilst the bottom waters below 3.5 metres remained undisturbed.

2.3 Water chemistry

Water samples for the analysis of Chlorophyll-a were collected weekly from the 20. April 2020 from surface (-0.5 m) water at station 3 (Fig. (Søndergaard et al., 2005). A volume of water ranging from (0.2 to 1 litre) was filtered and the GFC papers preserved for chlorophyll-a analysis, which were determined spectrophotometrically after ethanol extraction (Jespersen and Christoffersen, 1987) and alkalinity was measured weekly by gran titration (Søndergaard et al., 2005). Depth profiles of temperature, electrical conductivity (EC) and dissolved oxygen (DO) were measured manually with an Aqua TROLL 500 probe from every -0.5 or -1 m down to -5 m depth).

2.4 Greenhouse gas sampling

2.4.1 Dissolved concentration

Samples of dissolved concentrations of CH_4, CO_2 and N_2O were collected weekly from the 20. April 2020 from surface waters and weekly from surface and bottom water from the 26. May 2020 to the 13. October 2020. The samples were taken using head-space equilibration after (Mcauliffe, 1971), where 20 ml of water was collected from just below the water surface and 20 ml of N_2 was introduced as a headspace in a 60-ml syringe and then shaken vigorously for one minute. The 20 ml headspace was then transferred to a 12-ml pre evacuated glass vial.

Gas concentrations in the headspace were determined on a dual-inlet Agilent 7890 GC system interfaced with a CTC CombiPal autosampler (Agilent, Nærum, Denmark) (Petersen et al., 2012). For the GC, certified CO_2, CH_4 and N_2O standards were used for calibration and validation. Aqueous concentrations in N_2O, CH_4 and CO_2 were calculated from the headspace gas concentrations according to Henry's law and using Henry's constant corrected for temperature and salinity (Weiss, 1974; Weiss and Price, 1980; Wiesenburg and Guinasso, 1979). A recent study (Koschorreck et al., 2021) identified significant bias in the estimate of CO_2 concentrations using headspace equilibration at lower concentrations. We applied their correction using separately measured alkalinity as described in Koschorreck et al. (2021).

The fluxes of N_2O, CH_4 and CO_2 between the water and the overlying atmosphere were estimated as

$$f_g = k_g\left(C_{wat,g} - C_{eq,g}\right)$$

Where $f_g$is the flux of a specific gas g, k_g is the piston velocity of the gas and $C_{wat,g} - C_{eq,g}$ is the gradient of concentration between the concentration of gas dissolved in the water ($C_{wat,g}$) and the concentration of gas the water would have at equilibrium with the atmosphere ($C_{eq,g}$).

We calculated a gas transfer velocity k_{600} for each sampling occasion using the relationship based on windspeed described in (Cole and Caraco, 1998).

$$k_{600} = 2.07 + 0.215U_{10}^{1.7}$$

U_{10} is the mean daily windspeed at 10m (m s^{-1}) obtained from the Danish meteorological institute (DMI;20x20 km grid data)

$$k_g = k_{600}\left(\frac{Sc_g}{600}\right)^x$$

Sc_g is the Schmidt number(Wanninkhof, 1992) of the specific gas *g*. We chose x =-2/3 as this factor is used for smooth liquid surface (Deacon, 1981).

Daily flux rates were calculated using linear interpolation of the weekly surface measurements from each of the sampling points. The diffusive surface water fluxes were calculated by taking an average of the daily flux rate from the 12. May 2020 to the 13. October 2020 for each location. Then an average of the 3 locations was multiplied by the area of the lake and the number of days covered by the study, here 126 days was chosen to match the period over which ebullition was measured.

The total content of the gases in the lake's bottom waters were calculated from the dissolved concentration of the gases multiplied by an estimate of the volume of the water in the hypolimnion. The volume of water in the hypolimnion was estimated from the lake profiles manually conducted on the day of sampling. The top of the hypolimnion was determined by the depth below which oxygen was less than 0.5 mg l^{-1}. A detailed bathymetry of the lake allows the calculation of the area and therefore volume of water that lies below a given depth.

During the study period two major turnover events occurred, the process of lake turnover and full mixing can take a number of days, and the outgassing even longer. The oxygen data, from the buoy, indicated

that it can take up to four days and this provides time for CH_4 oxidation to occur (Søndergaard et al., 2023b). In order to estimate the amount of CH_4 oxidised over the course of the multiple days of degassing we directly measured CH_4 oxidation rates in the surface waters of the lake. This was done in June 2023 in five locations in this lake using methods outlined in (Thottathil et al., 2019) where five water samples from five different locations and each was incubated over 4 days with and the change in CH_4 concentration used to calculate oxidation rates. We used the minimum (0.267 µg CH_4-C l^{-1} h^{-1}), mean (0.44 µg CH_4-C l^{-1} h^{-1}) and maximum (0.58 µg CH_4-C l^{-1} h^{-1}) oxidation rates to estimate the range of CH_4 oxidation likely to have occurred over the course of the two main turnover events. Assuming that the degassing took four days, these rates would consume between 2 and 8% of the CH_4 contained in the hypolimnion. Using the mean oxidation value the turnover fluxes were reduced by 4.1% on the 30th of June 2020 and by 6% for the 25th August 2022.

2.4.2 Ebullition

The ebullitive flux of CH_4 was estimated using at total of 40 floating chambers placed on 4 transects of 10 chambers each (Fig. 1). The chambers have a volume of 8 litre and a surface area of 0.075 m^2, similar to those used by (Bastviken et al., 2015). As the existing literature indicated that ebullition is lower as water depth increases (Wik et al., 2013) the transects were placed to maximise the measurement of the low end of the depth gradient on the shallower slopes of the western end of the lake (Fig. 1). The average and maximum depth of each transect was T1: 293 cm and 472 cm; T2: 181 cm and 267, T3: 223 cm and 300 cm and T4 166 cm and 220 cm.The chambers were set on the 14. May 2020 and sampled every two weeks from that date, and on one occasion after one week until September 17th, which is a period of 127 days. Twenty ml of sample was taken from the floating chamber and injected into a pre-evacuated 12 ml vial (exetainer, Labco). Gas concentrations were determined on the same GC than described above (Petersen et al., 2012)

Ebullitive flux of CH_4 was estimated as:

211 $$\frac{p_{gas} \times Vol_{bub}}{t \times A}$$

212 Where p_{gas} is the concentration of CH_4 in the gas that was trapped, Vol_{bub} is the volume of the chamber
213 (i.e. 7L), t is the time during which the samples was collected and A is the area of chamber (i.e. 0.075 m^2).
214 A portion of the CH_4 released via ebullition in the chamber will have re-dissolved in the water or might
215 leak through the chamber walls, thus underestimating the ebullitive flux. We have made a number of
216 measurements to constrain this error and to compare estimates based on static chambers with other
217 approaches. The result show that whilst static chambers underestimate ebullition, given the temporal
218 variability of ebullition, static chambers continually deployed provide a better estimate of average ebullition
219 than short term (24-48 hours) deployment using portable gas monitors or flushing chambers.
220
221 Therefore, whilst static chambers method cannot be said to accurately quantify CH_4 emissions, they can be
222 relied upon to compare differences in ebullition between time periods, with the caveat that they are always
223 an underestimate of actual ebullitive flux.
224
225 Total ebullitive flux from the lake was calculated by taking a mean of the emissions from each transect over
226 the 126 day period. Then taking an average of the means of four transects and multiplying this by the time
227 of deployment of the chambers in days, which was 126 days, and by the area of the lake. This gives a total
228 ebullitive flux of CH_4 for the lake over the period of measurement from May to mid-September.
229
230 The three different flux types, surface diffusion, ebullition and turnover emission were then converted in
231 comparable units of total lakes emissions (as g or kg of gas) over the studied period and also converted into
232 CO_2-equivalents using a conversion factor related to their 100 year global warming potential (GWP) of 28
233 for CH_4 and 265 for N_2O.
234
235 **2.5 Statistical methods**

To test for a significant difference among the emissions from the stratified and mixed phase we used generalised least squares (GLS) with a variance function to account for heterogeneity of variance between the phases. In the case of the ebullitive flux, as the collected phase often covered periods including both mixed and stratified phases there were three categories, mixed, stratified and both mixed and stratified. All analysis was carried out in R version 4.2.1 (R Development Core Team, 2022) and the GLS used the package nlme (Pinheiro et al., 2014).

3.0 Results

3.1 Lake physical and chemical characteristics

Depth profiles measured weekly from April show that stratification was initiated by the 26. May 2020 this may have broken down briefly and established again, visible in the temperature sensors for the buoy on the 5. June 2020 (Fig. 2). There were then 12 days of mixing followed by stable period of stratification with onset the 14. June 2020 and a duration of 16 days until a mixing event around the 30. June 2020. The following two weeks had cooler water and a mixed water column, herafter a ca. 6 day period of stratification from the 15. to 21. July 2020. A mixed phase of two weeks then followed until stratification reestablished on 4. August 2020 and persisted until the end of August, partial mixing is indicated by the buoy data from the 21. August 2020, but the weekly manual profile to deeper water inidcate that full mixing did not occur until after the 25. August 2020. The effects of the stratification and mixing events on the high frequency DO data measured at -3.8 m are clear, with rapid deoxygenation occuring after the onset of stratification and oxic bottom waters returning when the lake mixed (Fig, 2). The pattern in chlorophyll-a also follow, to some degree, those of stratification, with the exception of early spring. Chlorophyll-a values were extremely high in spring peaking at the start of June 2020 and falling gradually (Fig. 2). (Søndergaard et al., 2023b)During the periods of stratification chlorophyll biomass was lower,

and when a mixing event occurred the values increased, which is particularly evident in the July mixing periods (Fig. 2).

3.2 Concentrations of dissolved gases and fluxes from the surface waters.

The concentrations of the dissolved gases showed great variation from near or below atmospheric concentrations in some cases and up to an extremely high concentration (over 5 mg CH_4 C l^{-1}) in the bottom waters on the 30. June 2020. There was some spatial heterogeneity in the surface waters, with the more littoral locations showing the greatest variation and the highest values (Figs. 3,4,5). In particular the most littoral zone, where the water was shallower around 1 m in depth, showed the highest values just prior to, or coincident with, the stratification turnover. Table 2 shows the mean diffusive flux of each gas over the sampling period along with the mean flux in mixed and stratified phases. For CO_2 there was a lot of temporal variation in flux dynamics, though not a large difference between mixed and stratified phases in terms of mean values (Table 2). There were some periods of CO_2 influx in spring and later summer and these tended to coincide with the end of a mixed phase and the start of the stratification phase. Nitrous oxide concentrations were generally low (Figs 4 & 5) with the lake being a source of N_2O in the spring period and a sink or a very small source thereafter. The CH_4 concentration in the surface waters (Fig. 3) and the calculated diffusive emissions are relatively low, but did increase in the stratification periods with higher average values (Table 2 & Fig. 6). There was also some spatial variation with higher CO_2 and CH_4 diffusive emissions in the shallower sampling locations, both in stratified and mixed conditions (Fig. 6).

The most marked patterns in GHG concentration were evident in the bottom waters sampled at -4.5 m, which accumulated to very large concentrations of CO_2 but particularly CH_4 in the periods of stratification (Fig. 3 & 4). The ratio of CO_2 to CH_4 is illustrative in highlighting how stratification has altered the biogeochemical processes in the hypolimnion with CH_4 production becoming more prevalent. .

For example on 30. June 2020 after 16 days of stratification the the ratio CO_2:CH_4 in the bottom waters was 0.8, whereas 7 days later after the mixing event it was 187 at the same depth.

3.3 Ebullitive fluxes

The CH_4 bubble flux, presented here as mean values for each of the 4 transects, ranged from 0.303 to 81.1 mg CH_4 C m^2 d^{-1} for the individual transect over the growing season measurement. There is a very clear, statistically significant impact of stratification on the ebulltive efflux of CH_4 with stratified periods showing significantly markedly higher levels of emission (Fig. 7 and Table 2). In addition, there was a difference in average emissions among the different transects, with those with lower average water depth (T2 & T4) having lower emission than the transects with chambers over deeper water (T1 & T3) (Fig. 7). The samples collected from the chambers reflect two weeks of bubble and diffusion collection and the quantification of the flux is therefore an average of the period of chamber deployment, which was two weeks, or in one case a single week (Fig. 7). This two week period on occasion covered both stratified and mixed phases and on these occassions efflux was intermediate between purely mixed and stratified periods (Table 2 and Fig. 7).

3.4 Total lake fluxes

Scaling up the results to total flux of gases from the whole lake over the period of study and including the estimated emissions from two turnover events show a very different effect of stratification on the balance of types of emissions for the three gases. The majority of CH_4 emission (56%) result from the two short-lived turnover events (Fig. 8), whereas their contribution to CO_2 and N_2O emission was 5% and 1% respectively.

Fluxes of CO_2 and N_2O were mostly diffusive, which represtented 95% of emissions of both gases. Methane diffusive flux was 14% of total emission, whereas CH_4 ebulltion was more than twice as much at

29% of total CH_4 emission. In terms of global warming potential CO_2 and CH_4 emission were comparable, but the contribution of the turnover efflux was the dominant factor for CH_4 emissions.

4. Discussion

This study set out to assess the role of thermal stratification on the GHG dynamics in a lake undergoing frequent but temporary stratification. We found that the emission of the three GHGs showed different degrees of variation between the mixed and stratified phases. The largest and most significant variation was in CH_4 ebullition (Table 2), whilst the difference in diffusive fluxes, though marked for CH_4 was not significant. The mean of the total emissions from Ormstrup in the stratified phase (59.9 mg CH_4-C m^{-2} day^{-1}) corresponds relatively closely to the mean of the total emissions (ebullition plus diffusion) reported for lakes in this size range (47 mg CH_4-C m^{-2} day^{-1}) from a paper synthesising multiple studies (Rosentreter et al., 2021). The mean emissions for the whole period (26.6 CH_4 -C m^{-2} day^{-1}) were lower than Rosentreter et al. (2021) but similar to other studies with mean emissions of 30.9, 20.7 and 22.7 CH_4 -C m^{-2} day^{-1} and were reported by Peacock et al. (2021), Sø et al. (2023) and Peacock et al. (2019) respectively. Whereas the average CO_2 (504 mg CO_2-C m^{-2} day) at Ormstrup was lower than 993.5 1 mg CO_2-C m^{-2} day^{-1} measured by Peacock et al. (2021) but higher than the 264.6 and 205.1 mg CO_2-C m^{-2} day^{-1} measured by Sø et al. (2023) and Peacock et al. (2019) respectively. The different temporal resolution and duration of these studies, eleven single day sampling from April to December (Peacock et al., 2021), five days continuous sampling on one occasion in late September (Sø et al., 2023) and a single early summer snapshot (Peacock et al., 2019) make direct comparison difficult. The data here do, however, provide a clear answer to the question of how thermal stratification effects GHG dynamics in shallow eutrophic lakes with an increase in total emissions (diffusion, ebullition and turnover) during the stratified period (Table 2, Fig 9). Previous work, combining observations and modelling suggested the opposite patterns (Bartosiewicz et al., 2019) as the shielding effect of the stratification results in cooler bottom waters which reduces CH_4 production due to the process being temperature dependent

(Bartosiewicz et al., 2016). This strong shielding effect may apply in deeper lakes experiencing more stable stratification, or less eutrophic lakes. The result here from a relatively shallow eutrophic lake, indicate that temporary stratification causes increases in GHG emissions. **4.1 Diffusive fluxes**Diffusive emissions did not, on average, show a strong stratification effect (Table 2). In particular variation in N_2O emissions did not match patterns of stratification, with emissions more directly related to nitrate concentrations (Audet et al., 2020), as reflected by the fact the lake is a sink of N_2O in late summer when nitrate was below detection limits for several weeks. There were peaks in emission of CH_4 and CO_2 at the end of stratification periods, particularly in the shallower water sampling points (Fig. 6). There were periods of influx of CO_2, which coincided somewhat with periods of stratification, but the pattern was not consistent as other factors, for example, chlorophyll-a concentration also play a role.

Littoral zones can have markedly different GHG dynamics to deeper zones due to shallower water having lower pressure (Wik et al., 2013), less time for CH_4 oxidation (Bastviken et al., 2008) or abundant plants which influence a range of biogeochemical processes (Davidson et al., 2018; Esposito et al., 2023). It is therefore possible that littoral zone dynamics could cause these differences. However, the increase occurred at all three sampling points at the end of June 2020, which indicates a lake-wide driver and the peak may represent the start of mixing after stratification. Strong winds were measured on the 29th and 30th June 2020 (Søndergaard et al., 2023b) coincident with these increased littoral emissions. These winds would have caused lateral movement of the surface water causing an upwelling of bottom water, rich in CH_4 and CO_2, in the littoral margins at the opposite end of the lake. Thus, whilst we do not have direct evidence it seems more likely that these increased emissions in the littoral zone were driven, at least in part, by the upwelling of GHG rich bottom waters.

4.2 Ebullitive fluxes

In contrast to the diffusive flux, the ebullitive emission of CH_4 shows a very clear response to stratification with an order of magnitude difference in emissions between periods where the sampling reflected purely mixed or stratified periods (Table 2 & Fig. 7). The two-week resolution of the sampling meant that some samples covered both stratified and mixed phases and these samples had intermediate fluxes, as they cover both low (mixed) and high emission (stratified) periods. The spatial variation in ebullition is also illustrative of the impacts of stratification and the role of anoxia in shaping CH_4 fluxes. The two transects with the largest mean and maximum depths (T1 and T3) had the largest emissions, with the deeper of the two (T1) having the highest emissions and showing the largest relative increase during the stratification phases. This pattern is different to that found some other studies where bubble emissions were larger in shallower water (Wik et al., 2013), although in this, and another study (Sø et al., 2023), there was in increase in bubble flux in deeper water in late summer. The deeper water at Ormstrup experienced anoxia early in season resulting in locations with deeper water having higher ebullition rates than shallower areas. This is at odds with ideas stemming from the metabolic theory of ecology stating that temperature (Yvon-Durocher et al., 2014) in particular at the sediment surface (Bartosiewicz et al., 2019) can be used to predict CH_4 efflux. Whilst CH_4 production is temperature dependent at the cellular level, CH_4 emissions were rather independent of the sediment temperature, for example in the first two weeks of July 2020 emissions were low and the sediment surface temperature was relatively high. Thus, temperature alone is a poor predictor of ecosystem scale CH_4 emissions.

It should be noted that the methods used to estimate bubble flux here, where floating chambers are sampled every two weeks is a “less than perfect method”, which in nearly all cases will underestimate ebullitive flux. Logistical and financial constraints make continual sampling difficult and here we balanced these constrains against the greater time required to apply more accurate methods, such as bubble traps (Wik et al., 2013), automatic flushing chambers (Bastviken et al., 2015). Such is the variability of bubble flux in space and time that using measurement from a shorter period of 1-2 days can result in a larger error in estimation of emissions than results from the longer term deployment of a static

chamber (see supplementary materials 1 and 2). The results in figure 7 show that sampling a single week a year or even more regular monthly sampling of a shorter duration would be unlikely to accurately characterise ebullition. Bubble traps have been used on longer terms but in eutrophic systems they can suffer extensive biofouling which can impede their use. Thus, the continuous monitoring of ebullition using static chamber with known biases was deemed the least worst method available, but we acknowledge that ebullitive emissions are underestimated. We further acknowledge that this approach of static chambers should, where possible, be replaced by other methods to estimate ebullition, such as automatic flushing chambers. It is difficult to compare the mean values of emission with other studies as there are different scales of measurement both in space and time. However, comparing the values for ebullition recorded here with other longer-term studies carried out in lakes using bubble traps (Burke et al., 2019; Delsontro et al., 2016), shows higher values recorded at Ormstrup lake compared with other lakes, but lower values that have been measured in ponds (Ray and Holgerson, 2023; Delsontro et al., 2016), the latter being known to have higher emissions of CH_4 (Holgerson and Raymond, 2016).

4.3 Turnover fluxes

In addition to the diffusive and ebullitive emissions, the turnover flux, which consists of the gases accumulated in the hypolimnion being released on turnover, was also estimated, with a correction of CH_4 oxidation applied. There were two major turnover events at the end of June and in late in August 2020, which were preceded by 16 and 22 days of stratification, respectively. It was not possible to directly-measure turnover flux, as they are relatively discrete events where the efflux likely occurs over the course of a few hours, or a few days (Søndergaard et al., 2023b). Thus, the efflux estimation is based on a series of assumptions and thus must be treated with caution. Notwithstanding this uncertainty, we can be confident the turnover flux represents a very large proportion of the total emission of CH_4 emissions from Ormstrup Lake over the growing season. We estimate it contributed more than 50 % of growing season CH_4 emissions and 5 % of CO_2 emissions. This highlights a very significant, and difficult to measure,

409 contribution to GHG emissions from lakes undergoing temporary stratification, which are among the
410 most common lake type in Denmark (Søndergaard et al., 2023a).

411

412 **4.1 Stratification effects**

413 The results here suggest that GHG dynamics were driven both directly and indirectly by the stratification
414 patterns and the anoxia it induced in the bottom waters. At Ormstrup Lake the thermal stratification of the
415 water column quickly led to anoxia, with only a matter of hours to days for the oxygen to be consumed
416 once the bottom waters were isolated (Fig. 2). The ratios of CO_2:CH_4 evidence how this promotes CH_4
417 over CO_2 production in the stratification phase (see Fig 9). In addition to promoting CH_4 production such
418 conditions would preclude, or severely limit, oxic CH_4 oxidation, which has the potential to consume a
419 large proportion of CH_4 produced in the anoxic sediments (Bastviken et al., 2008), though anoxic
420 consumption of CH_4 can still occur (Blees et al., 2014). The raw emission data do not provide any direct
421 information on the balance of production versus oxidation, but the CO_2:CH_4 suggest there was marked
422 shift to conditions where methanogenesis was the dominant process and there was reduced CO_2
423 production. Studies have shown that CH_4 oxidation can consume large proportions of the CH_4 produced
424 under hypoxia (Saarela et al., 2019) and it is possible that there is intense CH_4 oxidation occurring at the
425 thermocline during the periods of stratification at Ormstrup lake , but this was not directly measured at the
426 lake. In addition to the more direct effects of anoxia there may be some indirect effects of the patterns of
427 stratification and mixing that promote greater GHG emissions. Søndergaard et al. (2023b) recently
428 reported how nutrient dynamics at Ormstrup Lake were altered by the lake stratification and full details
429 can be found there, of relevance here is the impact on chlorophyll-a which saw a large spring peak after
430 which the abundance tracked the stratification and mixing regime, with a lag time. There was a general
431 reduction, or at least no increase as the stratification period progressed, perhaps due to nutrient limitation
432 in the epilimnion. Upon mixing there was generally an increase in chlorophyll-a, though the weekly
433 sampling resolution makes this difficult to assess. Chlorophyll-a and the labile dissolved organic carbon

(DOC) that result from abundant chlorophyll-a have been shown to be associated with higher diffusive and ebullitive CH_4 emissions (Davidson et al., 2015; Beaulieu et al., 2019; West et al., 2012; Zhou et al., 2019). It is not possible to say here whether a stable summer long stratification would have led to decreased chlorophyll-a as nutrients became limiting due to their isolation in the bottom waters and reliable high frequency chlorophyll-a data are required to convincingly demonstrate this phenomenon. Notwithstanding these uncertainties it may be the case that the temporary stratification, interspersed with mixing events, observed here represents a 'sweet spot' providing both the resources, i.e. chlorophyll-a and the labile DOC it produces, and optimal conditions (anoxia) for CH_4 production.

Predicting climate change effects on GHG emissions in a future warmer world is not straightforward, as there are multiple interacting drivers which combine to shape the GHG emissions of lakes. However, this study suggests that temporary stratification, which is increasingly recognised as prevalent in ponds and shallow lakes (Holgerson et al., 2022) and is likely to become more common with continued climate change impacts (Woolway and Merchant, 2019) is likely to increase GHG emissions. This will be particularly the case in more eutrophic systems where abundance algal derived dissolved organic matter can fuel CH_4 production (Zhou et al., 2019).

The combination of high frequency data on water temperature and dissolved oxygen combined with weekly measurements of GHGs increase the reliability of the findings presented here. Up until relatively recently it has been assumed that for shallow lakes, such as Ormstrup lake, stratification is not an important feature. Sampling has therefore focused on the surface layers of water bodies, using dissolved concentrations of gases or floating chambers to characterise flux, e.g. (Davidson et al., 2015; Audet et al., 2020; Peacock et al., 2021). Thus, most studies have overlooked bottom waters and do not have the temporal resolution required to capture turnover flux emissions from surface measurements. Furthermore, whilst many studies now include estimates of bubble emissions of CH_4 e.g. (Bergen et al., 2019), the necessary temporal resolution to accurately characterise ebullitive emission is not well established. The

finding here indicated that in such dynamic systems near continuous measurement is desirable and that short term collection over one or two days could provide massive, over or underestimate of CH_4 ebullition.

Our results show very large temporal variation in emissions of all three gases, but in particular CO_2 and CH_4, and this highlights the need for high frequency measurements to accurately characterize emissions from lakes. Even the weekly frequency of the sampling in this study was not sufficient to directly measure all the emission pathways and turnover flux had to be inferred from bottom water calculations. These data show that to capture the extent of GHG emissions from lakes it is vital we include all forms of flux, including ebullition and turnover flux. Recent work has highlighted the fact that most emissions of CH_4 (over 50%) from fresh waters come from highly variable systems (Rosentreter et al., 2021), with the mean and median emission rates of CH_4 differing greatly, indicating a few large emitters are responsible for a large proportion of emissions. The sampling frequency applied here is rare, if a more standard resolution of monthly measurements was applied the emissions estimate of all the gases, but in particular CH_4, would be highly dependent on what phase of the stratification was captured. As an example, a monthly sampling frequency could potentially miss all the stratification peaks - consequently massively underestimating emissions, whereas a different sampling frequency could catch a number of peaks and give a much higher estimate. Thus, the same sampling frequency on the same lake, but timed differently could lead to conclusions of highly variable emissions. Consequently, in these highly dynamic systems where temporary stratification occur in summer, high frequency measurements are required to accurately estimate emissions. This is possible through eddy covariance approaches capable of capturing short term changes and covering a large area (Erkkilä et al., 2018) but the cost of these systems means they are not scalable to many sites. An increasingly accessible alternative is the use of automatic flushing chambers using low cost sensors (Bastviken et al., 2020), which provide the potential for affordable high spatial and temporal resolution measurement of GHG dynamics. This is a requisite for understanding the drivers of

GHG dynamic, which is required for being able to predict how they will respond in a range of scenarios related to land use, climate change and management interventions.

Code/data availability

The datasets generated during and/or analysed during the current study are not publicly available as they form part of ongoing research projects but are available from the corresponding author on reasonable request and will be made publicly available later in the research project.

Author contributions

MS secured the funding for the wider lake restoration research project supplying the data. TAD, MS and JA conceptualized the gas study. TAD and AN established the buoy and sensor system. EL, CE, TAD, TB and JA collected and analysed the data. TAD wrote the paper and all authors commented on earlier versions and read and approved the final draft.

Competing interests

The authors declare that they have no conflicts of interest.

Acknowledgement

We thank our splendid technician team of Lene Vigh, Malene Kragh, Dorte Nedergaard and Dennis Hansen for their extreme competence on the lab and the field. We acknowledge Theis Kragh for the depth map of the lake already published in Søndergaard et al. 2023. We are very grateful to the Poul Due Jensen Foundation for providing great support for this work and the Ormstrup project generally. TAD and CE were also supported by GREENLAKES (No. 9040-00195B) and The European Union's Horizon 2020 research and innovation programmes under grant agreement No 869296—The PONDERFUL Project.

513 Table 1. Summary lake information, summer mean values and (standard deviation) of a range of

514 variables

Variable	n	Year 2020
Secchi depth (m)	22	0.86 (0.28)
Chlorophyll a (µg/l)	20	53.4 (28.9)
pH	22	8.04 (0.77)
Total phosphorus (mg/l)	22	0.58 (0.11)
Total nitrogen (mg/l)	22	1.50 (0.41)

515

516 Table 2. Mean greenhouse gas flux (units CO_2: mg CO_2-C m^{-2} day^{-1}, N_2O: mg N_2O -N m^{-2} day^{-1}, CH_4 both

517 diffusive and ebullitive in mg CH_4-C m^{-2} day^{-1}) from the lake from spring to Autumn 2020. The emissions

518 are divided in diffusive, ebullitive emissions. The mean values for all the surface water stations and all

519 four transects of chambers are given. Emissions area separated into mixed versus stratified phases and

520 there SD are also given. Ebullition was collected for a period covering two weeks so on a number of

521 occasion covered both mixed and stratified periods thus ebullition has a third category where both

522 mixed and stratified conditions occurred is given. Ebullition was significantly different across the three

523 phases, diffusive fluxes were not significantly different for *p* values of 0.05.

524

525

526

Emission type	gas	mean	mixed	Stratified	Strat and mixed
Diffusive	CO_2	493.7 (*529.6)*	559.6 *(433.1)*	449.8 *(587.6)*	
	CH_4	9.47 *(16.0)*	5.9 *(4.1)*	12.7 *(20.2)*	
	N_2O	0.11 *(0.09)*	0.09 *(0.08)*	0.12 *(0.11)*	
Ebullition	CH_4	17.28 *(19.62)*	**4.84** ***(3.44)***	**47.29** ***(21.95)***	**12.74** ***(10.34)***

527

528

529 Figure legends

530 Figure 1. Ormstrup lake bathymetry and sampling stations for surface water greenhouse gas sampling
531 (St1, St2, St3) bottom waters were sampled at S3. Transects of 10 bubble traps were placed on T1- T4.
532 Adapted from the Søndergaard et al. 2023.

533 Figure 2 Temperature profile from June 2020 when the buoy was deployed and surface and bottom water
534 oxygen from June to the end of September 2020. Manual chlorophyll-a ($\mu g\ L^{-1}$) values are also given in
535 the top panel.

536 Figure 3. Dissolved CH_4 concentrations from surface and bottom waters – thermal stratification periods
537 highlighted in grey and the white background indicate mixed waters

538 Figure 4 . Dissolved CO_2 concentrations from surface and bottom waters–thermal stratification periods
539 highlighted in grey and the white background indicate mixed waters

540 Figure 5 Dissolved N_2O gas concentrations surface and bottom thermal stratification periods highlighted
541 in grey and the white background indicate mixed waters

542 Figure 6. Omstrup lake surface fluxes of the CH_4, CO_2 and N_2O gases based on dissolved conentration ,
543 thermal stratification periods highlighted in grey and the white background indicate mixed waters

544 Figure 7. Plot of CH_4 ebullition averaged for each transect (10 chambers per transect), data collected from
545 40 traps every two weeks. Thermal stratification periods highlighted in grey and the white background
546 indicate mixed waters.

547 Figure 8 – Total lake emissions per gas over the growing season in CO_2 equivalents. The emissions are
548 divided different emission modes: Diffusive, ebullitive and turnover flux. All estimates constain some
549 uncertainty, in particular ebulltive flux is an underestimate and the turnover flux also contains a gret deal
550 of uncertainty.

551 Figure 9. Summary of the quantities of the gases present in the water and the volumes emited from the
552 different pathways. The size of the arrow is proportional to the emissions from each pathway and with the
553 startified state on the left and the mixed state on the right, with the turnover flux in the centre.

554

555 Figures and legends

556 Figure 1.

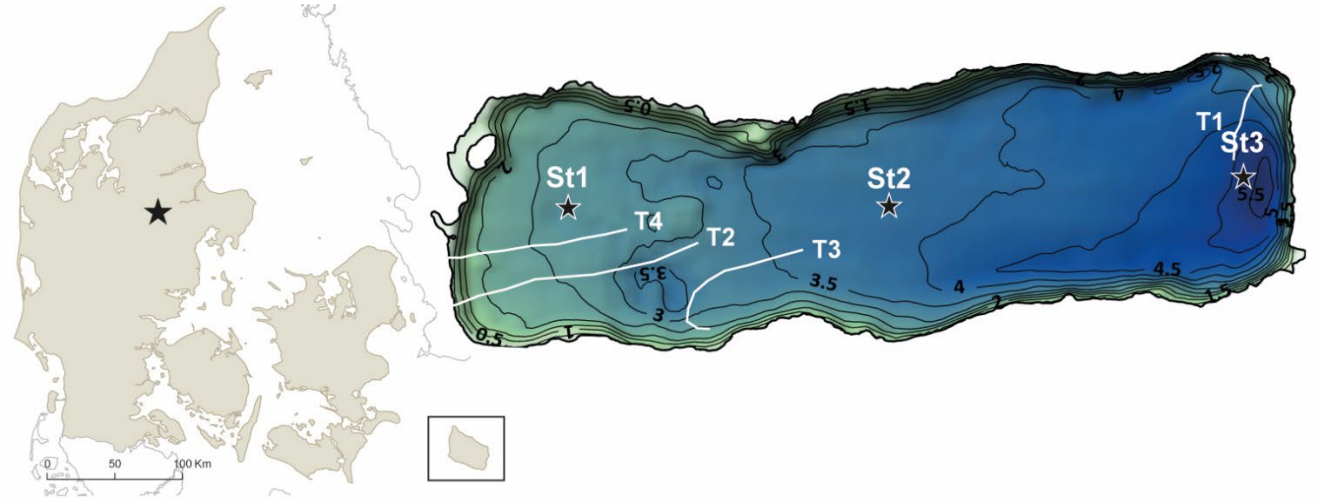

557

558 Figure 1. Ormstrup lake bathymetry and sampling stations for surface water greenhouse gas sampling (S1,
559 S2, S3) bottom waters were sampled at S3. Transects of 10 bubble traps were placed on T1- T4. Adapted
560 from the Søndergaard et al. 2023.

561

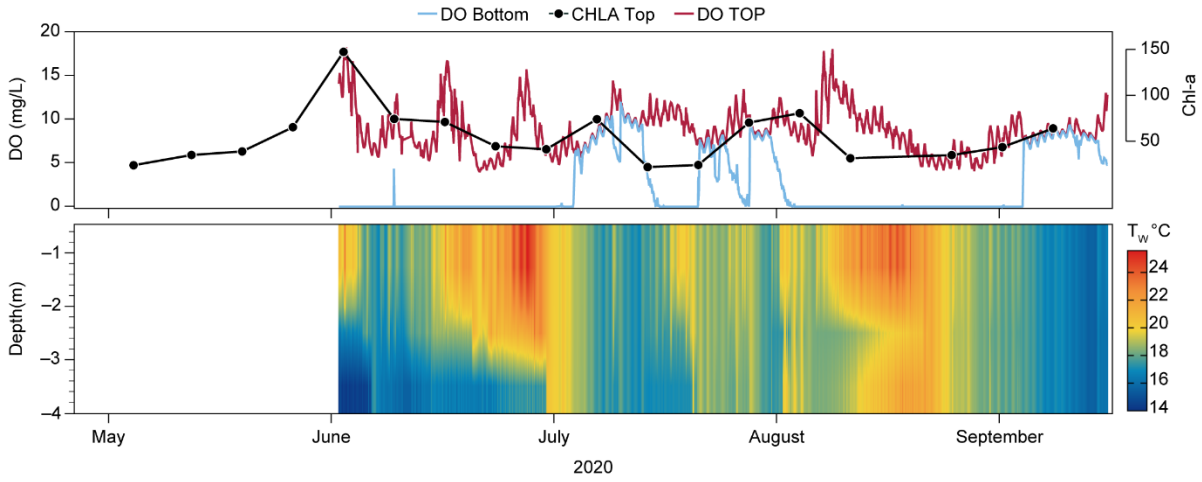

562

563 Figure 2 Temperature profile from June when the buoy was deployed and surface and bottom water
564 oxygen from June to the end of September. Chlorophyll-a (µg L^{-1}) values are also given in the top panel
565 and surface (DO TOP) and bottom (DO Bottom) dissolved oxygen (mg L^{-1}) are also given

566

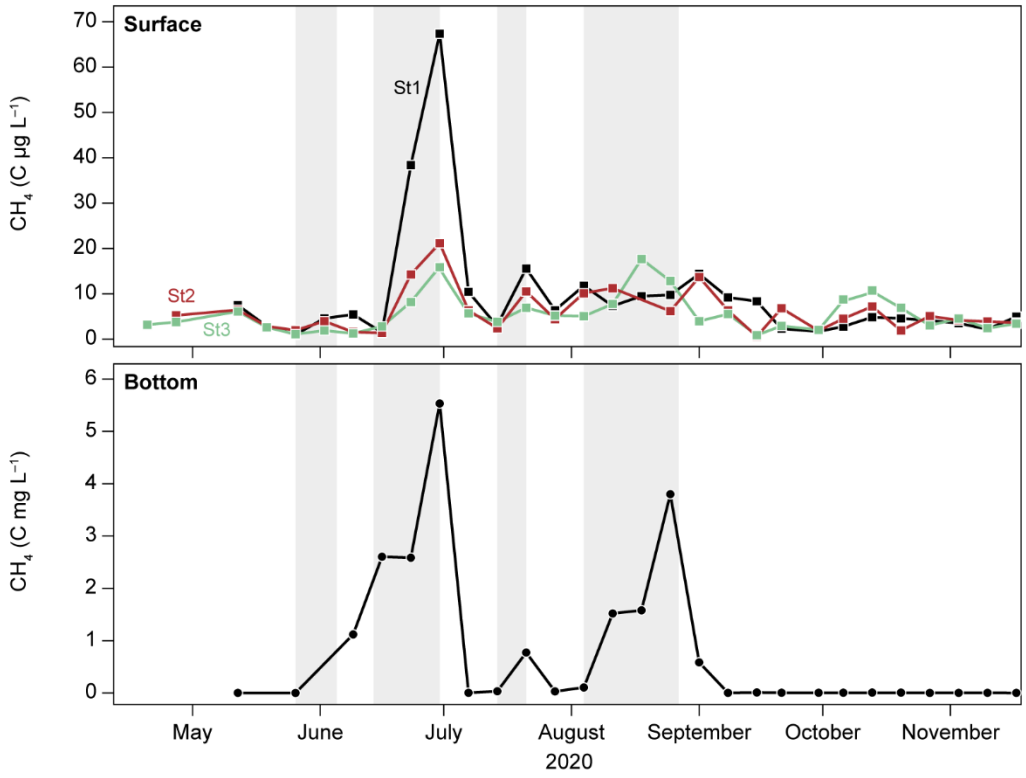

Figure 3. Dissolved CH_4 concentrations from surface and bottom waters – thermal stratification periods highlighted in grey; white background indicate mixed waters. Note different y axis scales

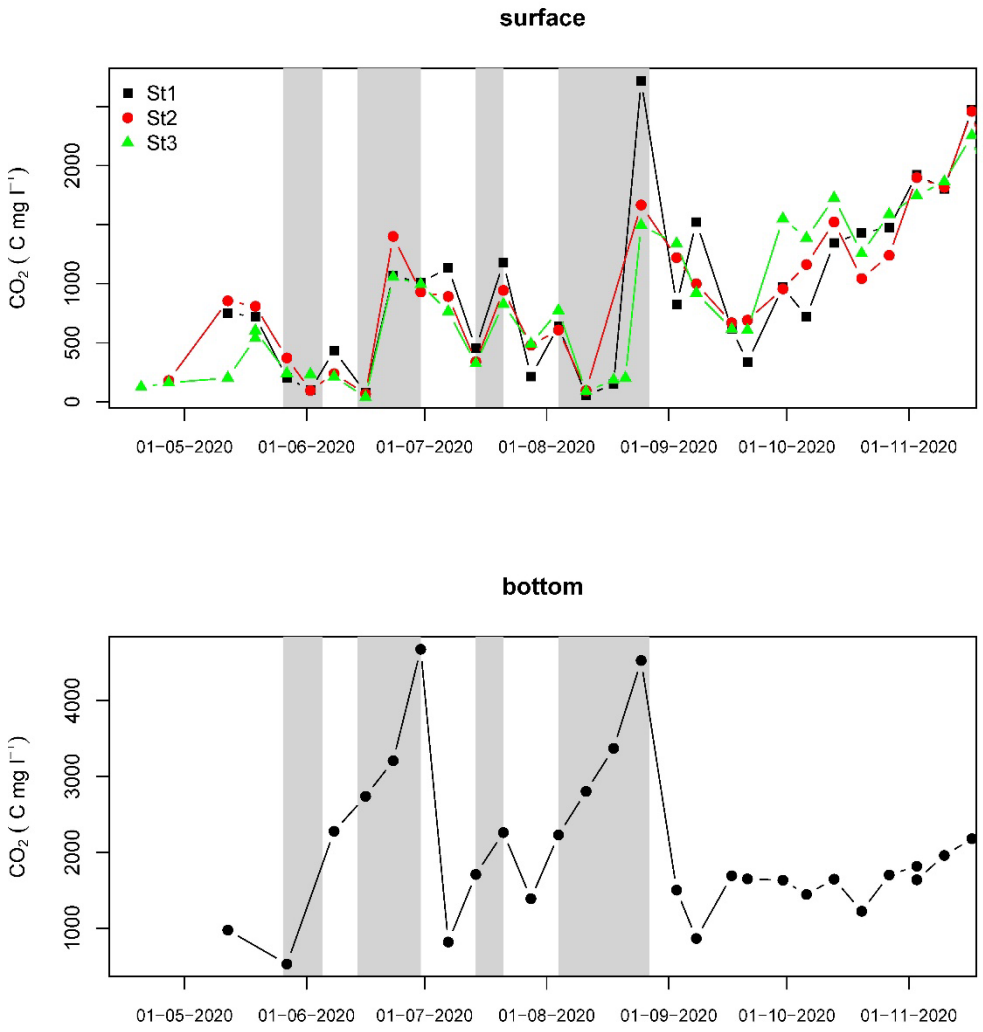

570

571 Figure 4 . Dissolved CO_2 concentrations from surface and bottom waters–

572 thermal stratification periods highlighted in grey; white background indicate mixed waters

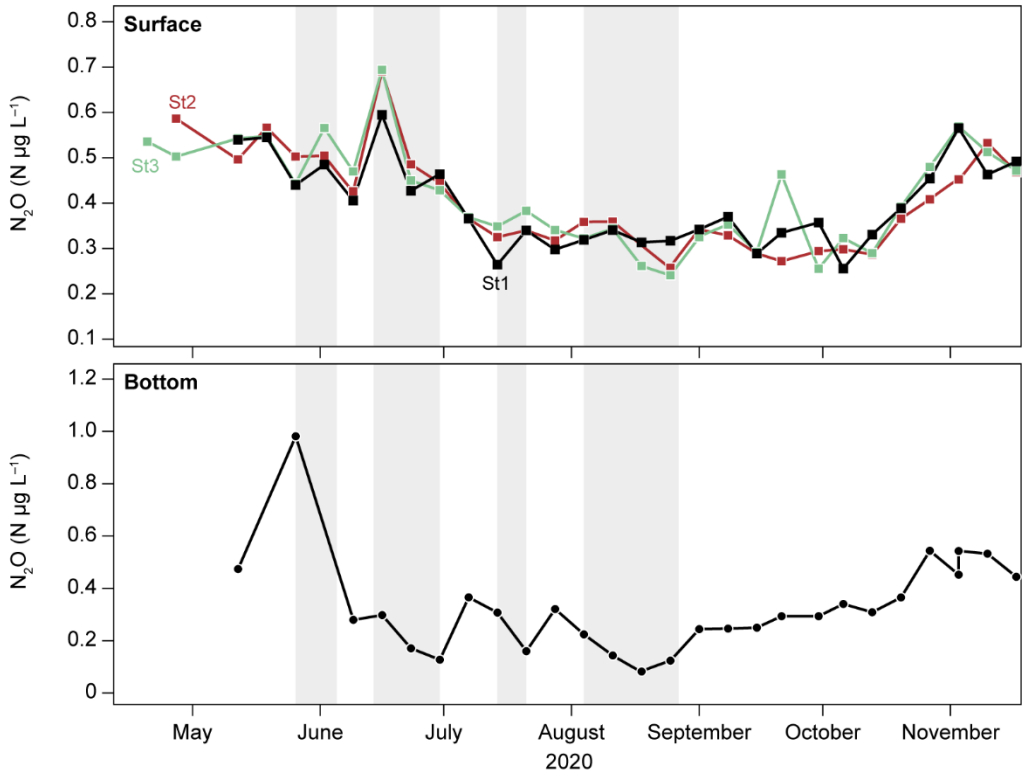

573

574 Figure 5 Dissolved N_2O gas concentrations surface and bottom thermal stratification periods highlighted

575 in grey; white background indicate mixed waters

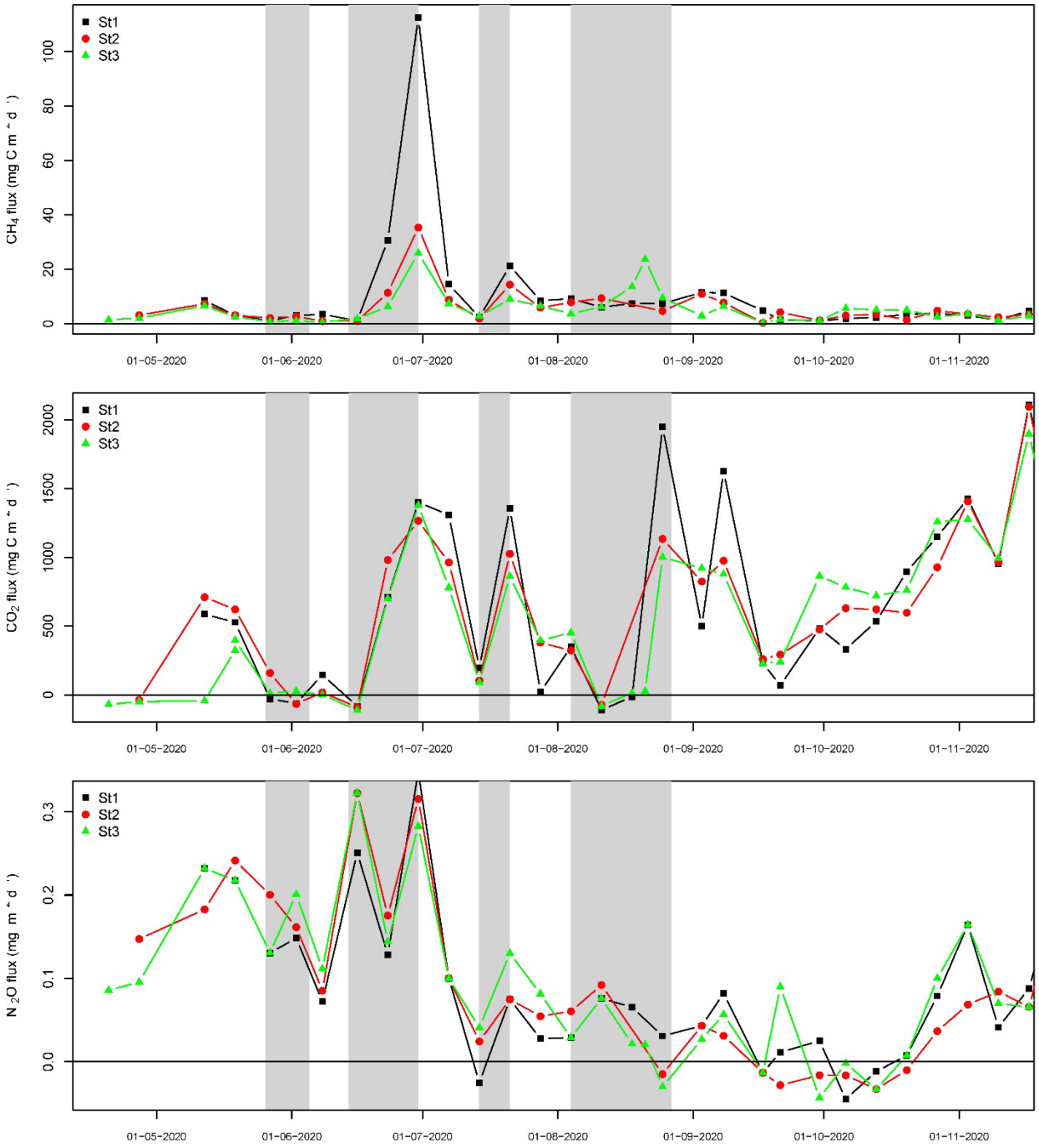

Figure 6. Omstrup lakesurface fluxes of the CH_4, CO_2 and N_2O gases based on dissolved conentration , thermal stratification periods highlighted in grey; white background indicate mixed waters

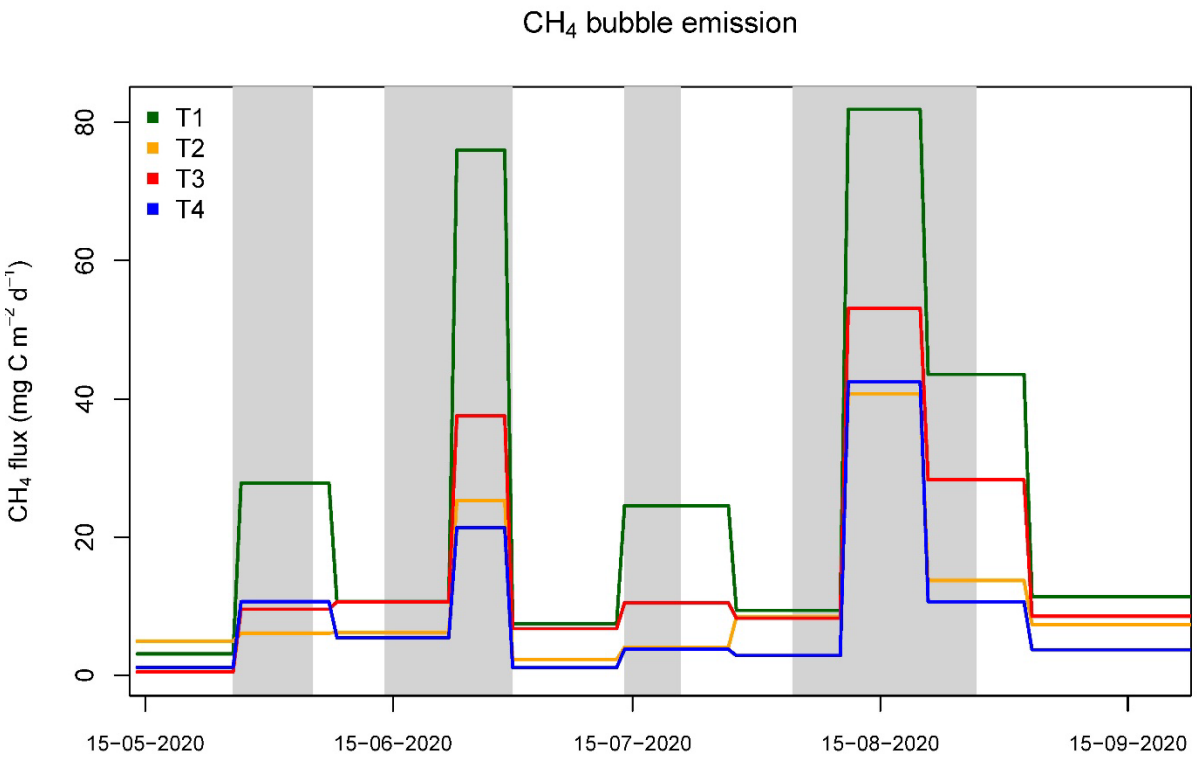

Figure 7. Plot of CH_4 ebullition averaged for each transect (10 chambers per transect), data collected from 40 traps every two weeks. thermal stratification periods highlighted in grey; whitle background indicate mixed waters.

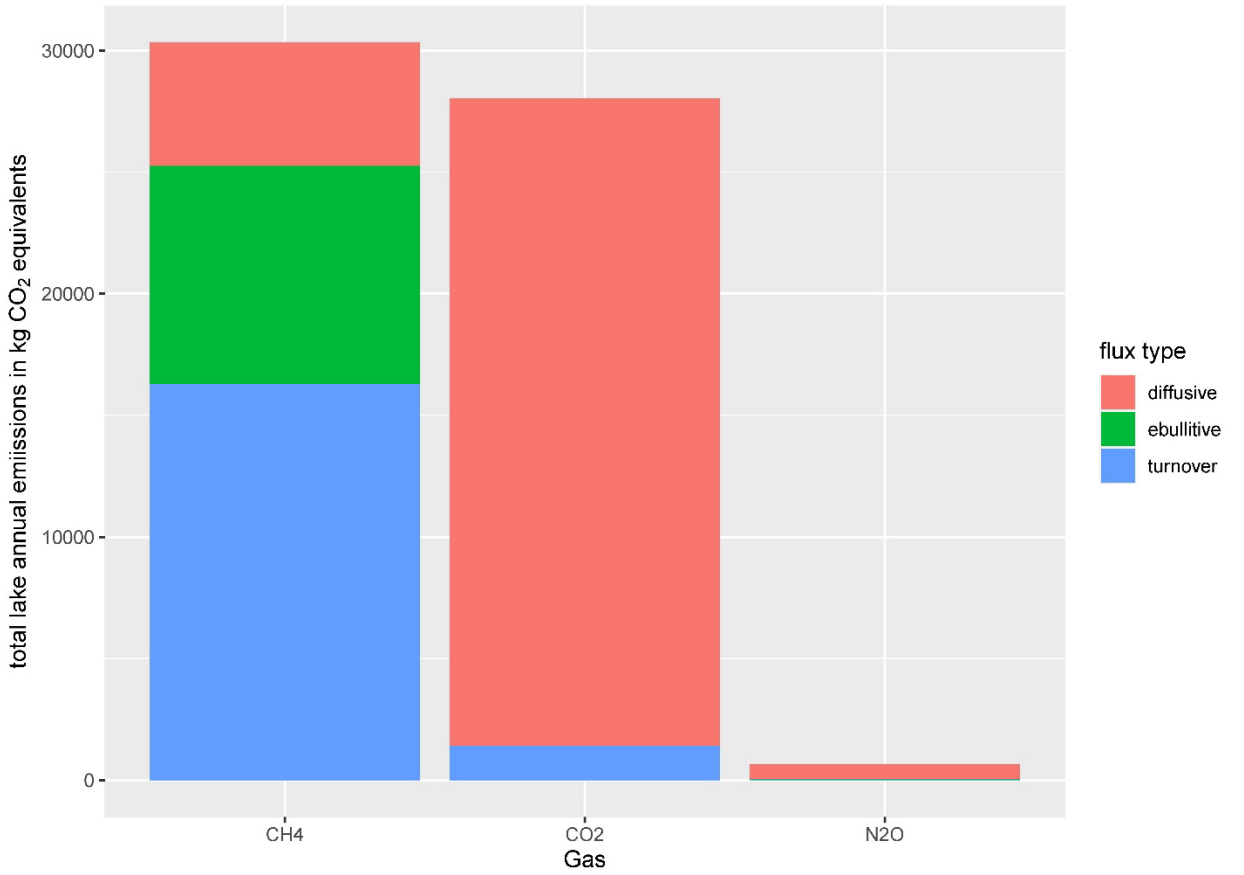

586

587 Figure 8 – Total lake emissions per gas over the growing seasson in CO_2 equivalents. The emissions are

588 divided different emission pathways: Diffusive, ebullitive and turnover flux.

589

590

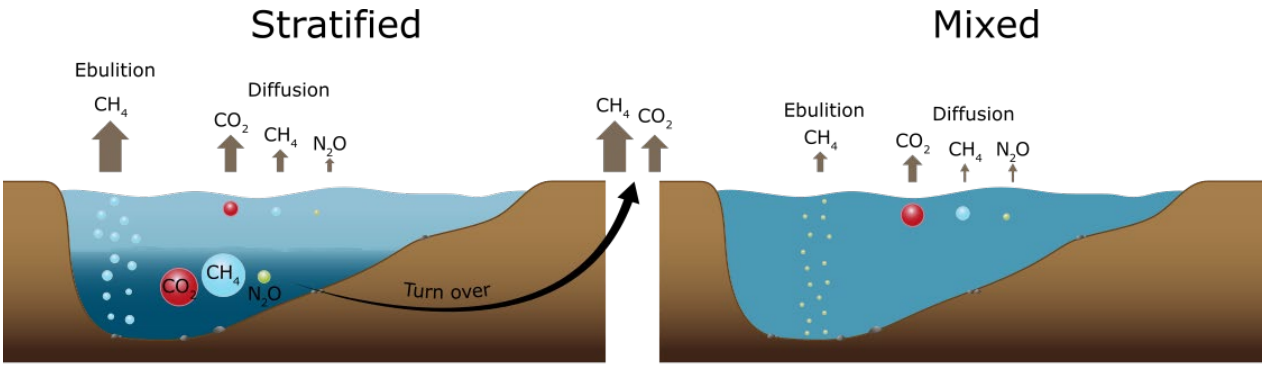

591

592 Figure 9 Summary of different flux types (bubble, diffusive and turnover) for the main greenhouse gases

593 (CH_4 CO_2 and N_2O) observed between the stratified and mixed phases at Ormstrup lake patterns in the

594 stratified and mixed phase. The turnover flux of CH_4 and CO_2 is also represented. The size of the arrow

595 represents the relative amount of emission and the size of the circle in the lake represents the
596 concentration of dissolved gases in stratified or mixed water column.
597

598

References

Aben, R. C. H., Barros, N., van Donk, E., Frenken, T., Hilt, S., Kazanjian, G., Lamers, L. P. M., Peeters, E. T. H. M., Roelofs, J. G. M., de Senerpont Domis, L. N., Stephan, S., Velthuis, M., Van de Waal, D. B., Wik, M., Thornton, B. F., Wilkinson, J., DelSontro, T., and Kosten, S.: Cross continental increase in methane ebullition under climate change, Nat. Comms., 8, 1682, https://doi.org/10.1038/s41467-017-01535-y, 2017.

Audet, J., Carstensen, M. V., Hoffmann, C. C., Lavaux, L., Thiemer, K., and Davidson, T. A.: Greenhouse gas emissions from urban ponds in Denmark, Inland Waters, 1-13, https://doi.org/10.1080/20442041.2020.1730680, 2020.

Bartosiewicz, M., Laurion, I., and MacIntyre, S.: Greenhouse gas emission and storage in a small shallow lake, Hydrobiologia, 757, 101-115, https://doi.org/10.1007/s10750-015-2240-2, 2015.

Bartosiewicz, M., Laurion, I., Clayer, F., and Maranger, R.: Heat-Wave Effects on Oxygen, Nutrients, and Phytoplankton Can Alter Global Warming Potential of Gases Emitted from a Small Shallow Lake, Environ. Sci. Technol., 50, 6267-6275, https://pubs.acs.org/doi/10.1021/acs.est.5b06312, 2016.

Bartosiewicz, M., Przytulska, A., Lapierre, J.-F., Laurion, I., Lehmann, M. F., and Maranger, R.: Hot tops, cold bottoms: Synergistic climate warming and shielding effects increase carbon burial in lakes, Limnol. Oceanogr. Lett., 4, 132-144, https://doi.org/10.1002/lol2.10117, 2019.

Bastviken, D., Cole, J. J., Pace, M. L., and Van de Bogert, M. C.: Fates of methane from different lake habitats: Connecting whole-lake budgets and CH4 emissions, J. Geophys. Res., 113, G02024, https://doi.org/10.1029/2007JG000608, 2008.

Bastviken, D., Nygren, J., Schenk, J., Parellada Massana, R., and Duc, N. T.: Technical note: Facilitating the use of low-cost methane (CH4) sensors in flux chambers – calibration, data processing, and an open-source make-it-yourself logger, Biogeosciences, 17, 3659-3667, https://doi.org/10.5194/bg-17-3659-2020, 2020.

Bastviken, D., Sundgren, I., Natchimuthu, S., Reyier, H., and Gålfalk, M.: Technical Note: Cost-efficient approaches to measure carbon dioxide fluxes and concentrations in terrestrial and aquatic environments using mini loggers, Biogeosciences, 12, 3849-3859, https://doi.org/10.5194/bg-12-3849-2015, 2015.

Bastviken, D., Treat, C. C., Pangala, S. R., Gauci, V., Enrich-Prast, A., Karlson, M., Gålfalk, M., Romano, M. B., and Sawakuchi, H. O.: The importance of plants for methane emission at the ecosystem scale, Aquat. Bot., 184, 103596, https://doi.org/10.1016/j.aquabot.2022.103596, 2023.

Beaulieu, J. J., DelSontro, T., and Downing, J. A.: Eutrophication will increase methane emissions from lakes and impoundments during the 21st century, Nat. Comms., 10, 1-5, https://doi.org/10.1038/s41467-019-09100-5, 2019.

Bergen, T. J. H. M., Barros, N., Mendonça, R., Aben, R. C. H., Althuizen, I. H. J., Huszar, V., Lamers, L. P. M., Lürling, M., Roland, F., and Kosten, S.: Seasonal and diel variation in greenhouse gas emissions from an urban pond and its major drivers, Limnol. Oceanogr., 64, 2129-2139, https://doi.org/10.1002/lno.11173, 2019.

Blees, J., Niemann, H., Wenk, C. B., Zopfi, J., Schubert, C. J., Kirf, M. K., Veronesi, M. L., Hitz, C., and Lehmann, M. F.: Micro-aerobic bacterial methane oxidation in the chemocline and anoxic water column of deep south-Alpine Lake Lugano (Switzerland), Limnol. Oceanogr., 59, 311-324, https://doi.org/10.4319/lo.2014.59.2.0311, 2014.

Burke, S. A., Wik, M., Lang, A., Contosta, A. R., Palace, M., Crill, P. M., and Varner, R. K.: Long-Term Measurements of Methane Ebullition From Thaw Ponds, J. Geophys. Res. Biogeosci. . 124, 2208-2221, https://doi.org/10.1029/2018JG004786, 2019.

Cole, J.: Freshwater in flux, Nat. Geosci., 6, 13-14, https://doi.org/10.1038/ngeo1696, 2013.

Cole, J. J. and Caraco, N. F.: Atmospheric exchange of carbon dioxide in a low-wind oligotrophic lake measured by the addition of SF6, Limnol. Oceanogr., 43, 647-656, https://doi.org/10.4319/lo.1998.43.4.0647, 1998.
Davidson, T. A., Audet, J., Jeppesen, E., Landkildehus, F., Lauridsen, T. L., Søndergaard, M., and Syvaranta, J.: Synergy between nutrients and warming enhances methane ebullition from experimental lakes, Nat. Clim. Chang., 8, 156-160, https://doi.org/10.1038/s41558-017-0063-z, 2018.
Davidson, T. A., Audet, J., Svenning, J.-C. C., Lauridsen, T. L., Søndergaard, M., Landkildehus, F., Larsen, S. E., and Jeppesen, E.: Eutrophication effects on greenhouse gas fluxes from shallow-lake mesocosms override those of climate warming, Glob. Chang. Biol., 21, 4449-4463, https://doi.org/10.1111/gcb.13062, 2015.
Deacon, E. L.: Sea-air gas transfer: The wind speed dependence, Bound.- Layer. Meteorol., 21, 31-37, https://doi.org/10.1007/bf00119365, 1981.
Deemer, B. R. and Holgerson, M. A.: Drivers of Methane Flux Differ Between Lakes and Reservoirs, Complicating Global Upscaling Efforts, J. Geophys. Res. Biogeosci. . 126, e2019JG005600, https://doi.org/10.1029/2019JG005600, 2021.
DelSontro, T., Boutet, L., St-Pierre, A., del Giorgio, P. A., and Prairie, Y. T.: Methane ebullition and diffusion from northern ponds and lakes regulated by the interaction between temperature and system productivity, Limnol. Oceanogr., 61, S62-S77, http://doi.wiley.com/10.1002/lno.10335, 2016.
Erkkilä, K. M., Ojala, A., Bastviken, D., Biermann, T., Heiskanen, J. J., Lindroth, A., Peltola, O., Rantakari, M., Vesala, T., and Mammarella, I.: Methane and carbon dioxide fluxes over a lake: comparison between eddy covariance, floating chambers and boundary layer method, Biogeosciences, 15, 429-445, 10.5194/bg-15-429-2018, 2018.
Esposito, C., Nijman, T. P. A., Veraart, A. J., Audet, J., Levi, E. E., Lauridsen, T. L., and Davidson, T. A.: Activity and abundance of methane-oxidizing bacteria on plants in experimental lakes subjected to different nutrient and warming treatments, Aquat. Bot., 185, 103610, https://doi.org/10.1016/j.aquabot.2022.103610, 2023.
Holgerson, M. A. and Raymond, P. A.: Large contribution to inland water CO2 and CH4 emissions from very small ponds, Nat. Geosci., 9, 222-226, 2016.
Holgerson, M. A., Richardson, D. C., Roith, J., Bortolotti, L. E., Finlay, K., Hornbach, D. J., Gurung, K., Ness, A., Andersen, M. R., Bansal, S., Finlay, J. C., Cianci-Gaskill, J. A., Hahn, S., Janke, B. D., McDonald, C., Mesman, J. P., North, R. L., Roberts, C. O., Sweetman, J. N., and Webb, J. R.: Classifying Mixing Regimes in Ponds and Shallow Lakes, Water Resour. Res., 58, e2022WR032522, https://doi.org/10.1029/2022WR032522, 2022.
Jespersen, A. and Christoffersen, K.: Measurements of Chlorophyll a from phytoplankton using ethanol as extraction solvent., Archiv für Hydrobiologie, 109, 445-454, 1987.
Kirillin, G. and Shatwell, T.: Generalized scaling of seasonal thermal stratification in lakes, Earth Sci. Rev., 161, 179-190, https://doi.org/10.1016/j.earscirev.2016.08.008, 2016.
Koschorreck, M., Prairie, Y. T., Kim, J., and Marcé, R.: Technical note: CO2 is not like CH4 – limits of and corrections to the headspace method to analyse pCO2 in fresh water, Biogeosciences, 18, 1619-1627, 10.5194/bg-18-1619-2021, 2021.
McAuliffe, C.: Gas chromatographic determination of solutes by multiple phase equilibrium, Chem Technol, 1, 46-51, 1971.
Meerhoff, M., Audet, J., Davidson, T. A., De Meester, L., Hilt, S., Kosten, S., Liu, Z., Mazzeo, N., Paerl, H., Scheffer, M., and Jeppesen, E.: Feedbacks between climate change and eutrophication: revisiting the allied attack concept and how to strike back, Inland Waters, 1-42, https://doi.org/10.1080/20442041.2022.2029317, 2022.

691 Peacock, M., Audet, J., Jordan, S., Smeds, J., and Wallin, M. B.: Greenhouse gas emissions from urban
692 ponds are driven by nutrient status and hydrology, Ecosphere, 10, e02643,
693 https://doi.org/10.1002/ecs2.2643, 2019.
694 Peacock, M., Audet, J., Bastviken, D., Cook, S., Evans, C. D., Grinham, A., Holgerson, M. A., Högbom, L.,
695 Pickard, A. E., Zieliński, P., and Futter, M. N.: Small artificial waterbodies are widespread and persistent
696 emitters of methane and carbon dioxide, Glob. Chang. Biol., 27, 5109-5123,
697 https://doi.org/10.1111/gcb.15762, 2021.
698 Petersen, S. O., Hoffmann, C. C., Schäfer, C. M., Blicher-Mathiesen, G., Elsgaard, L., Kristensen, K.,
699 Larsen, S. E., Torp, S. B., and Greve, M. H.: Annual emissions of CH4 and N2O, and ecosystem respiration,
700 from eight organic soils in Western Denmark managed by agriculture, Biogeosciences, 9, 403-422,
701 https://doi.org/10.5194/bg-9-403-2012, 2012.
702 Pinheiro, J., Bates, D., DebRoy, S., Sarkar, D., and R Core Team: nlme: Linear and Nonlinear Mixed Effects
703 Models, 2014.
704 R Development Core Team: R: a language and environment for statistical computing. R Foundation for
705 Statistical Computing (4.2.1) [code], 2022.
706 Ray, N. E. and Holgerson, M. A.: High Intra-Seasonal Variability in Greenhouse Gas Emissions From
707 Temperate Constructed Ponds, Geophysical Research Letters, 50, e2023GL104235,
708 https://doi.org/10.1029/2023GL104235, 2023.
709 Rosentreter, J. A., Borges, A. V., Deemer, B. R., Holgerson, M. A., Liu, S., Song, C., Melack, J., Raymond, P.
710 A., Duarte, C. M., Allen, G. H., Olefeldt, D., Poulter, B., Battin, T. I., and Eyre, B. D.: Half of global methane
711 emissions come from highly variable aquatic ecosystem sources, Nat. Geosci., 14, 225-230,
712 https://doi.org/10.1038/s41561-021-00715-2, 2021.
713 Saarela, T., Rissanen, A. J., Ojala, A., Pumpanen, J., Aalto, S. L., Tiirola, M., Vesala, T., and Jäntti, H.: CH4
714 oxidation in a boreal lake during the development of hypolimnetic hypoxia, Aquat. Sci., 82, 19,
715 https://doi.org/10.1007/s00027-019-0690-8, 2019.
716 Schubert, C. J., Diem, T., and Eugster, W.: Methane Emissions from a Small Wind Shielded Lake
717 Determined by Eddy Covariance, Flux Chambers, Anchored Funnels, and Boundary Model Calculations: A
718 Comparison, Environ. Sci. Technol., 46, 4515-4522, https://doi.org/10.1021/es203465x, 2012.
719 Sø, J. S., Sand-Jensen, K., Martinsen, K. T., Polauke, E., Kjær, J. E., Reitzel, K., and Kragh, T.: Methane and
720 carbon dioxide fluxes at high spatiotemporal resolution from a small temperate lake, Sci. Total Environ.,
721 878, 162895, https://doi.org/10.1016/j.scitotenv.2023.162895, 2023.
722 Søndergaard, M., Jeppesen, E., Peder Jensen, J., and Lildal Amsinck, S.: Water Framework Directive:
723 ecological classification of Danish lakes, J. Appl. Ecol., 42, 616-629, https://doi.org/10.1111/j.1365-
724 2664.2005.01040.x, 2005.
725 Søndergaard, M., Nielsen, A., Johansson, L. S., and Davidson, T. A.: Temporarily summer-stratified lakes
726 are common: profile data from 436 lakes in lowland Denmark, Inland Waters, 1-14,
727 10.1080/20442041.2023.2203060, 2023a.
728 Søndergaard, M., Nielsen, A., Skov, C., Baktoft, H., Reitzel, K., Kragh, T., and Davidson, T. A.: Temporarily
729 and frequently occurring summer stratification and its effects on nutrient dynamics, greenhouse gas
730 emission and fish habitat use: case study from Lake Ormstrup (Denmark), Hydrobiologia, 850, 65-79,
731 https://doi.org/10.1007/s10750-022-05039-9, 2023b.
732 Thottathil, S. D., Reis, P. C. J., and Prairie, Y. T.: Methane oxidation kinetics in northern freshwater lakes,
733 Biogeochemistry, 143, 105-116, 10.1007/s10533-019-00552-x, 2019.
734 Wanninkhof, R.: Relationship between wind-speed and gas-exchange over the ocean, J. Geophys. Res.
735 Oceans, 97, 7373-7382, https://doi.org/10.1029/92jc00188, 1992.
736 Weiss, R. F.: Carbon dioxide in water and seawater: the solubility of a non-ideal gas, Mar. Chem., 2, 203-
737 215, https://doi.org/10.1016/0304-4203(74)90015-2, 1974.

738 Weiss, R. F. and Price, B. A.: Nitrous oxide solubility in water and seawater, Mar. Chem., 8, 347-359,
739 https://doi.org/10.1016/0304-4203(80)90024-9, 1980.
740 West, W. E., Coloso, J. J., and Jones, S. E.: Effects of algal and terrestrial carbon on methane production
741 rates and methanogen community structure in a temperate lake sediment, Freshw. Biol., 57, 949-955,
742 https://doi.org/10.1111/j.1365-2427.2012.02755.x, 2012.
743 Wiesenburg, D. A. and Guinasso, N. L.: Equilibrium solubilities of methane, carbon monoxide, and
744 hydrogen in water and sea water, J. Chem. Eng. Data . 24, 356-360,
745 https://doi.org/10.1021/je60083a006, 1979.
746 Wik, M., Crill, P. M., Varner, R. K., and Bastviken, D.: Multiyear measurements of ebullitive methane flux
747 from three subarctic lakes, J. Geophys. Res. Biogeosci. . 118, 1307–1321,
748 https://doi.org/10.1002/jgrg.20103, 2013.
749 Winslow, L., Read, J., Woolway, I., Brentrup, J., Leach, T., Zwart, J., Albers, S., and Collinge, D.:
750 rLakeAnalyzer: Lake Physics Tools: R package (1.11.4.1) [code], 2019.
751 Woolway, R. I. and Merchant, C. J.: Worldwide alteration of lake mixing regimes in response to climate
752 change, Nat. Geosci., 12, 271-276, https://doi.org/10.1038/s41561-019-0322-x, 2019.
753 Yvon-Durocher, G., Allen, A. P., Montoya, J. M., Trimmer, M., and Woodward, G.: The temperature
754 dependence of the carbon cycle in aquatic ecosystems, Adv. Ecol. Res., 43, 267-313,
755 https://doi.org/10.1016/B978-0-12-385005-8.00007-1, 2010.
756 Yvon-Durocher, G., Allen, A. P., Bastviken, D., Conrad, R., Gudasz, C., St-Pierre, A., Thanh-Duc, N., and del
757 Giorgio, P. A.: Methane fluxes show consistent temperature dependence across microbial to ecosystem
758 scales, Nature, 507, 488-491, https://doi.org/10.1038/nature13164, 2014.
759 Zhou, Y., Zhou, L., Zhang, Y., de Souza, J. G., Podgorski, D. C., Spencer, R. G. M., Jeppesen, E., and
760 Davidson, T. A.: Autochthonous dissolved organic matter potentially fuels methane ebullition from
761 experimental lakes, Water Res., 166, 115048, https://doi.org/10.1016/j.watres.2019.115048, 2019.
762